

Discovery of Novel HCN4 Blockers with Unique Blocking Kinetics and Binding Properties

SLAS Discovery
2021, Vol. 26(7) 896–908
© The Author(s) 2021



DOI: 10.1177/24725552211013824
journals.sagepub.com/home/jbx



Kosuke Nakashima^{1*}, Kenji Nakao^{2,3*}, and Hideki Matsui¹

Abstract

The hyperpolarization-activated cyclic nucleotide-gated 4 (HCN4) channel underlies the pacemaker currents, called “If,” in sinoatrial nodes (SANs), which regulate heart rhythm. Some HCN4 blockers such as ivabradine have been extensively studied for treating various heart diseases. Studies have shown that these blockers have diverse state dependencies and binding sites, suggesting the existence of potential chemical and functional diversity among HCN4 blockers. Here we report approaches for the identification of novel HCN4 blockers through a random screening campaign among 16,000 small-molecule compounds using an automated patch-clamp system. These molecules exhibited various blockade profiles, and their blocking kinetics and associating amino acids were determined by electrophysiological studies and site-directed mutagenesis analysis, respectively. The profiles of these blockers were distinct from those of the previously reported HCN channel blockers ivabradine and ZD7288. Notably, the mutagenesis analysis showed that blockers with potencies that were increased when the channel was open involved a C478 residue, located at the pore cavity region near the cellular surface of the plasma membrane, while those with potencies that were decreased when the channel was open involved residues Y506 and I510, located at the intracellular region of the pore gate. Thus, this study reported for the first time the discovery of novel HCN4 blockers by screening, and their profiling analysis using an automated patch-clamp system provided chemical tools that will be useful to obtain unique molecular insights into the drug-binding modes of HCN4 and may contribute to the expansion of therapeutic options in the future.

Keywords

hyperpolarization-activated cyclic nucleotide-gated 4 channel blockers, IonWorks, kinetics study, mutagenesis, homology modeling

Introduction

Hyperpolarization-activated cyclic nucleotide-gated (HCN) channels have a unique physiological property based on their unusual combination of hyperpolarization gating and poor selectivity between Na⁺ and K⁺. They underlie the native pacemaker currents, which are termed “If” in heart sinoatrial node (SAN) cells and “Ih” in nerve cells.^{1–4} These channels contribute to the control of the resting membrane potential and rhythmic activity of the excitable cells that express these channels.^{5–9} Four HCN subtypes have been identified and proposed as pharmacological targets to treat diseases such as heart failure, pain, and neurological disorders.^{5,7,10–13} Some HCN blockers have been identified through pharmacological exploitation and used to explore the molecular contributions of HCNs. Among them, HCN4 is predominantly expressed in the SAN cells of mammals and contributes to the heart beating.^{7,10,12} Thus, the development of blockers targeting HCN4 is thought to represent a

therapeutic approach to the treatment of several cardiac disorders associated with increased heart rate, such as hypertension, coronary artery disease, and heart failure.

Ivabradine, the most extensively studied HCN4 blocker, was clinically approved and has been used for the treatment

¹Neuroscience Drug Discovery Unit, Research, Takeda Pharmaceutical Company Limited, Fujisawa, Kanagawa, Japan

²Biomolecular Research Laboratories, Research, Takeda Pharmaceutical Company Limited, Fujisawa, Kanagawa, Japan

³Seedsupply Inc., Fujisawa, Kanagawa, Japan

*These authors contributed equally.

Received Dec 18, 2020, and in revised form March 17, 2021. Accepted for publication April 1, 2021.

Corresponding Author:

Hideki Matsui, Neuroscience Drug Discovery Unit, Research, Takeda Pharmaceutical Company Limited, 26-1, Muraoka-Higashi 2-chome, Fujisawa-shi, Kanagawa 251-8555, Japan.
Email: hideki.matsui@takeda.com

of heart failure and angina pectoris.^{14–17} Another HCN blocker, ZD7288, is structurally unrelated to ivabradine and has been used as a tool for studying the biophysical and physiological properties of these channels.^{18,19} Some of the conventional drugs used for treating arrhythmia and heart failure, such as lidocaine and carvedilol, have also been shown to provide HCN blockade.^{20,21} The mode of action of HCN blockers is diverse.²² For example, ivabradine accesses the inner surface of the pore of the human HCN4 channel from the cytoplasmic side when the channels are open and is thus called an “open-channel blocker”; moreover, the strength of its binding depends on the frequent change of direction of the ion flow that passes through the channels.^{23,24} Ivabradine blocks HCN1 as well as HCN4, and its blockade of mouse HCN1 requires the channels to be either in a closed state or in a transitional state between the open and closed configurations; however, the blockade does not occur when the channel is in an open state in contrast to its blockade of human HCN4.²³ Thus, ivabradine was classified as an open-channel blocker of hHCN4 channels and as a “closed-channel blocker” of mHCN1 channels, whereas ZD7288 is considered as an open-channel blocker, which is distinct from ivabradine because it is “trapped” in the closed state of mouse HCN1 in a current-dependent manner.²⁵ Lidocaine acts on HCN1 with a negative shift in $V_{1/2}$, decreased tonic and maximal currents, and slowed activation kinetics.²⁶ The discovery of such series of blockers with their various voltage-, current-, and state-dependent actions suggests the possibility of identifying other unique molecules, which will further help the understanding of HCN properties and drug discovery for HCN blockers.

For high-throughput screening (HTS) campaigns of ion-channel targets, fluorescence-based assays using ion-specific probes or membrane potential sensors are often employed because of a favorable combination of throughput, cost, and information content. However, such non-electrophysiology-based assays lack the accurate control of a membrane potential and resulted in failure in maintaining physiologically relevant states of voltage-gated channels.^{27–30} In fact, discrepancies have been observed between the results obtained from nonelectrophysiological and electrophysiological methods to study the voltage-gated ion channels; as a consequence, the nonelectrophysiological assays may generate false-negative hits including use-dependent blockers.^{31,32} Key profiling information, such as voltage and use dependence, cannot be approached in HTS campaigns without electrophysiological recordings. Recent advances in the automated patch-clamp technology have begun to break this bottleneck with high-quality, information-rich data and high-throughput capabilities.^{33–37} They can provide gating kinetics data of ion channels under physiological conditions controlled by voltage clamping, even in a 384-well format. Therefore, we can expect that these

technologies will provide an opportunity to identify novel molecules that modulate ion channels such as HCNs through HTS.

The focus of this article was to identify HCN4 blockers through the screening of 16,000 small-molecule compounds using an automated patch-clamp instrument, IonWorks, and to assess the blocking kinetics and binding properties of the HCN4 blockers compared with the previously reported blockers ivabradine and ZD7288.

Materials and Methods

Reagents

ZD7288 was purchased from Tocris Bioscience (Minneapolis, MN). Ivabradine was synthesized in-house. Our identified hit compounds, T-478 (*N*-[(2*S*)-1-([1,4'-bipiperidin]-1'-yl)-1-oxopropan-2-yl]-2,5-dichloro-4-methoxybenzene-1-sulfonamide), T-788((8*aR*)-1,1-diphenyl-7-[6-(1*H*-pyrazol-1-yl)pyridine-3-carbonyl]hexahydro-3*H*-[1,3]oxazolo[3,4-*a*]pyrazin-3-one), and T-524 (7-[3-(trifluoromethyl)phenyl]-1,2,3,4-tetrahydroisoquinoline), were synthesized in-house (see Fig. 3B).

Cell Preparation

Chinese hamster ovary (CHO) K1 cells expressing HCN4 (accession nos. AJ238850, Thr110Ser) were purchased from Cytomyx (San Francisco, CA). The HCN4 mutant genes (*C478A*, *Y506A*, and *I510A*) were cloned into the pIRES neomycin vector (Invitrogen, Carlsbad, CA). A Gene Pulser Electroporation System (Bio-Rad Laboratories Inc., Hercules, CA) was used to transfect CHOK1 cells with these plasmids. CHOK1 cells were maintained in Iscove's Modified Dulbecco's Medium (Invitrogen) supplemented with 10% dialyzed fetal bovine serum (Thermo Fisher, Waltham, MA), nonessential amino acids (Invitrogen), HT Supplement (Invitrogen), and 500 $\mu\text{g}/\text{mL}$ geneticin (Invitrogen). The cell lines at favorable proliferation stages were subcloned, resulting in 24–48 subclones that were screened to identify the best cell line based on the success rate of whole-cell formation and sufficient amplitude of the HCN4 current. All HCN4 cell lines were routinely maintained at 37 °C and incubated at 30 °C for 2–8 days prior to the electrophysiological measurements, to increase the functional expression of the HCNs.

Automated Patch-Clamp Recording in IonWorks

The IonWorks system (Molecular Devices, Sunnyvale, CA), which was originally described by Schroeder et al.,³⁸ was used to measure HCN channel activity. This system utilizes a planar patch-clamp technology with a 48-well parallel recording configuration and exploits robotic operation

for solution and cell handlings. The “patch-plate” technology of IonWorks employs a 384-well plate with a single hole in each well (SH mode) and 64 holes in each well (Population Patch Clamp [PPC] mode). To prepare the cells for the instruments, the cells were detached with versene (Invitrogen) and resuspended in culture medium and centrifuged at 500g for 2 min. The supernatant was removed and cells were resuspended in phosphate-buffered saline and centrifuged at 500g for 2 min. The supernatant was removed and cells were resuspended in external solution at a density of 1.5–3 million cells/3 mL, for loading onto IonWorks. Perforated (via 0.2 mg/mL amphotericin B solubilized in 0.36% DMSO) whole-cell recordings were performed in the device. Because the seal resistance in IonWorks is lower than that in the conventional patch-clamp methods, the system utilizes linear leak subtraction evaluated by a +10 mV prepulse from the holding potential at the beginning of the test protocol. In the test protocols, the holding potential was clamped at –30 mV and hyperpolarizing pulses were applied, the voltage and pulse number of which are described in each figure. Test compounds were automatically dispensed from a 96-well plate, which was prepared at threefold the final test concentrations because the test compounds were diluted by three times in the patch plate well (3.5 μ L of test compound was added to 7 μ L of the solution in the patch plate). Concentration–response tests were performed using 1:3 dilutions from the maximum concentration of the compound. The current triggered by voltage pulse was recorded prior to and 5–10 min after compound addition. The internal recording solution contained (in mM) K-gluconate (135), Na-gluconate (10), $MgCl_2$ (1.5), and HEPES (5), pH 7.3, as well as 50 μ g/mL amphotericin (Sigma, St. Louis, MO); and the external solution contained (in mM) Na-gluconate (115), KCl (30), $CaCl_2$ (1.5), $MgCl_2$ (0.5), and HEPES (5), pH 7.4.

Multiple Sequence Alignment

We performed multiple sequence alignment of the S6-P loop of hHCN4 (UniProtKB accession no. Q9Y3Q4) with the corresponding regions of mHCN2 (O88703.1), mHCN1 (O88704.1), and hERG (Q12809.1) using MAFFT version 7.0 (Multiple Alignment using Fast Fourier Transform).

Data Analysis

Current amplitudes were obtained from the raw traces recorded at the end of the last voltage pulse subtracted from the proximate baseline. In the experiments shown in **Figures 1 and 2** and the first half of the screening campaign using the SH mode, the success criteria of each well were set as (1) $>50 M\Omega$ in seal resistance at precompound measurement, (2) >200 nA in current amplitude at precompound measurement, (3) <200 nA in the dissociation of the

baseline between pre- and postcompounds, and (4) a 0.5- to 2.0-fold ratio in the seal resistance values between pre- and postcompounds. In the second half using the PPC mode, the success criteria were set as $>30 M\Omega$ in seal resistance at precompound measurement, and the others were the same as the SH mode. The measurement was always confirmed by a group of vehicle controls (0.3% DMSO) in all assays, thus ensuring assay performance on each plate. The test plates that did not meet the criterion (coefficients of variation $<15\%$) in the vehicle controls were reexamined. The success rate throughout the screening was 80%–95%. In the subsequent kinetic assessment (see **Fig. 4A,B**) using the PPC mode, the success threshold was raised as follows: (1) $>50 M\Omega$ and (2) >500 nA. The PPC mode was used for the C478A and Y506A mutants and the SH mode for the I510A mutant in the mutagenesis experiments. To evaluate compounds, percent inhibition values were calculated by the post-/preamplitude ratio in each well. A group of the sampling data was plotted as the mean value \pm standard deviation, as needed. To obtain concentration-dependent curves, percent inhibition values were plotted and fitted with a sigmoidal equation:

$$Y = 100 / (1 + 10^{((\text{LogIC}_{50X})\text{Slope}))}), \quad (1)$$

where Y is the percent inhibition, X is the log concentration, and Slope is the hill-slope factor calculated by a shared value for all data sets. To obtain the voltage-dependent activation curves presented in **Figure 1B**, steady-state currents were measured and normalized to the maximal current (I_{MAX}) and plotted as a function of the preceding membrane potential. The curves were fitted with the Boltzmann function as follows:

$$I = I_{\text{MIN}} + (I_{\text{MAX}} - I_{\text{MIN}}) / (1 + \exp((V_{1/2} - V) / \text{Slope})), \quad (2)$$

where I_{MIN} is the offset caused by a nonzero holding current and is not included in the current amplitude, V is the test potential, and $V_{1/2}$ is the midpoint of activation. Calculations, curve fittings, and panel drawing were performed using GraphPad Prism version 8.2.0 (GraphPad Software Inc., San Diego, CA).

Results

Using an automated patch-clamp system, IonWorks, HCN4 currents were successfully observed. **Figure 1A** (top) shows the voltage protocol used to induce a hyperpolarization pulse and the current traces obtained by the pulse application to the parent or HCN4-expressing CHO cells incubated at 30 or 37 $^{\circ}$ C before the measurements. Cell culture at

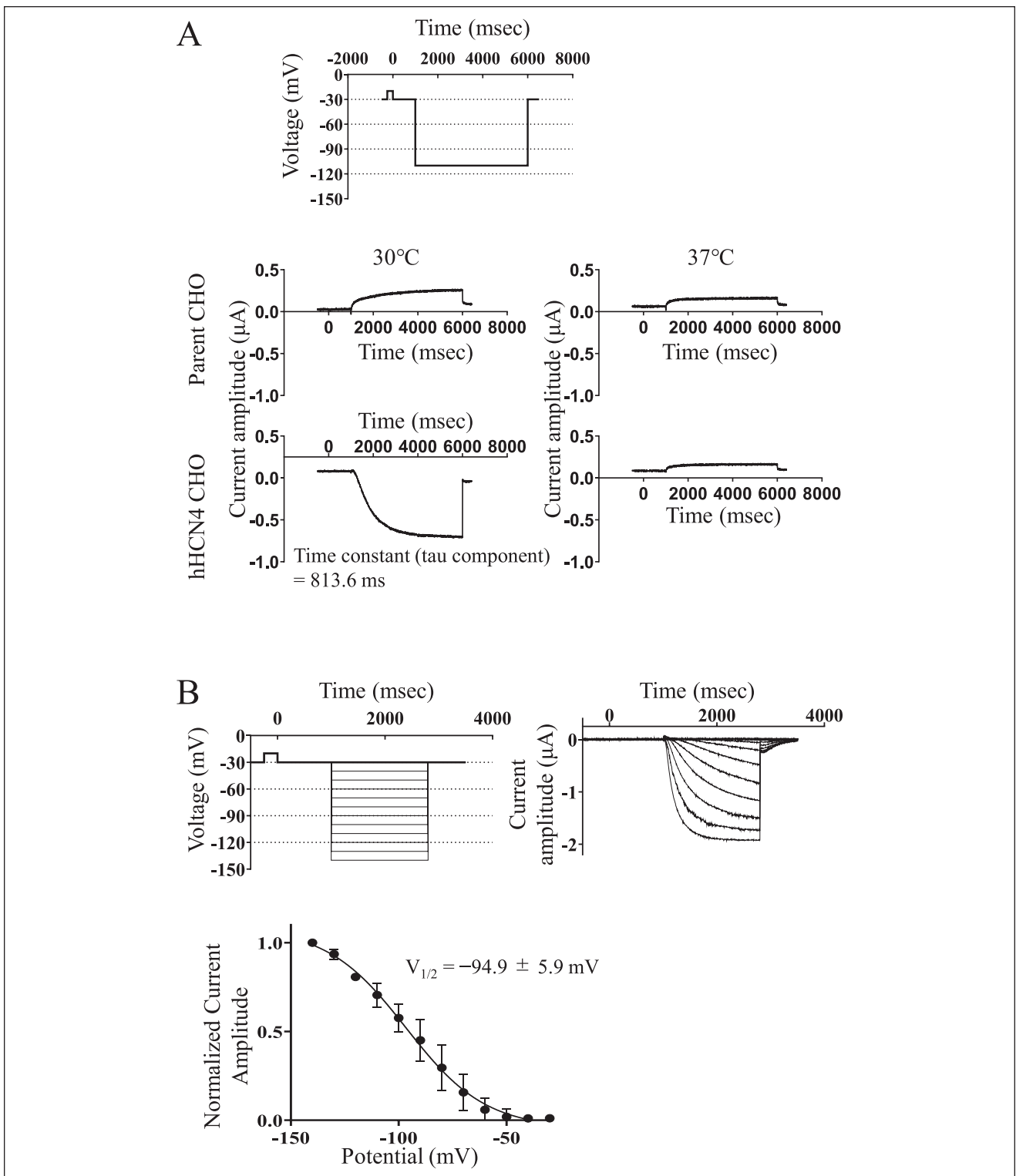


Figure 1. Studies of HCN4 currents recorded using IonWorks in an SH mode. **(A)** Voltage protocol (top) and typical current traces obtained from the parent (middle) and the human HCN4-expressing (bottom) CHO cells, which were incubated at 30 or 37 °C before measurements. **(B)** Voltage dependence of HCN4 activation. Voltage protocol (top left) and typical current traces (top right) are shown. The steady-state currents were normalized to the maximal current and plotted as a function of the preceding membrane potential. The curves were fitted with the Boltzmann function. The means \pm standard deviations from five experiments are indicated (bottom).

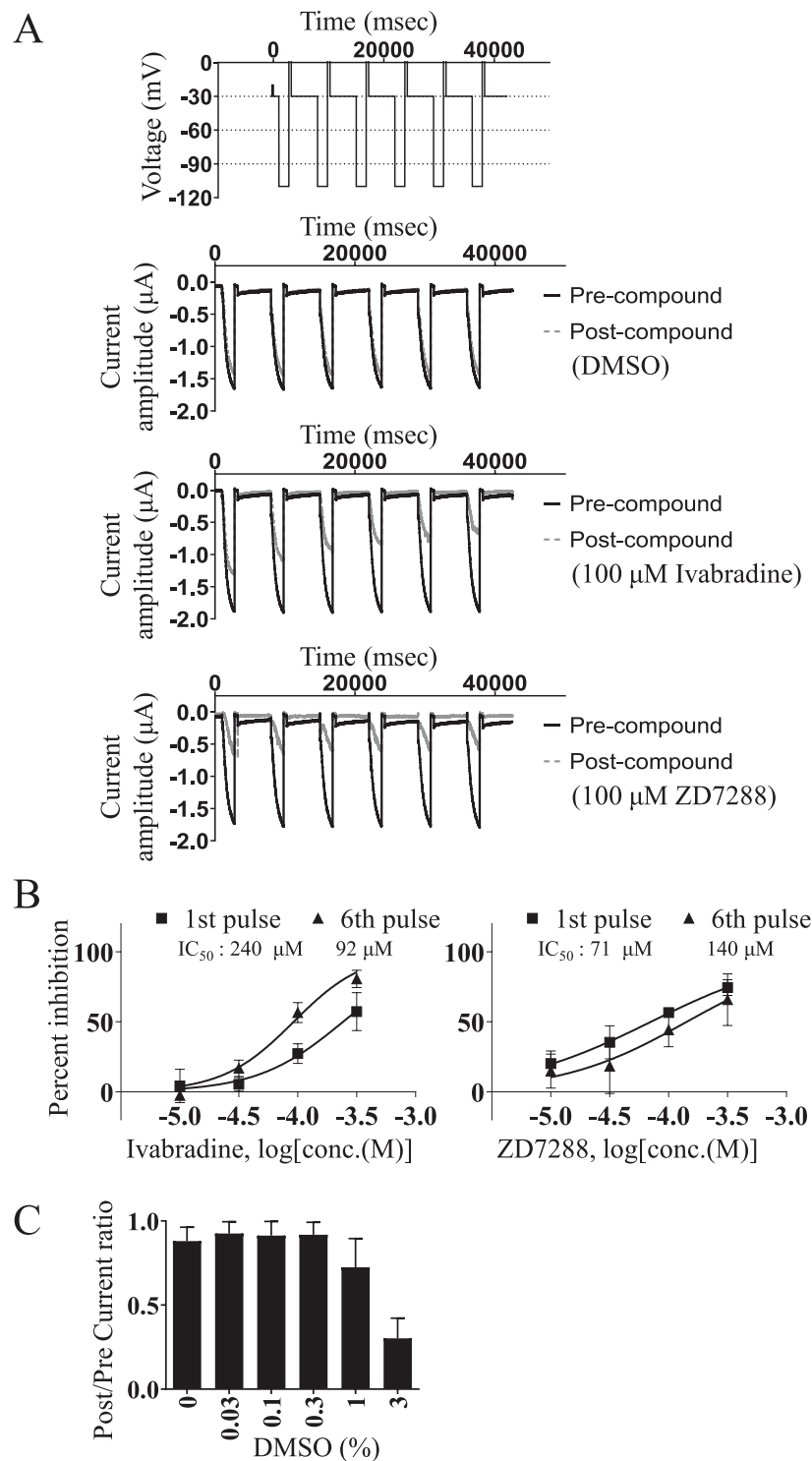


Figure 2. Blockade of the HCN4 channel by ivabradine and ZD7288 and DMSO tolerance test. **(A)** Voltage protocol (top) and typical current traces recorded before compound addition (precompound) and after the addition of each compound (postcompound). The traces obtained before and after the addition of DMSO (0.3%), ivabradine (100 μM), and ZD7288 (100 μM) are presented. **(B)** Concentration-dependent blockade of HCN4 current at the first and sixth hyperpolarizing pulses by ivabradine and ZD7288. The means \pm standard deviations from three experiments are indicated. The IC₅₀ values were determined by fitting the inhibition plots to a sigmoid equation (see “Data Analysis” section). **(C)** DMSO tolerance test in HCN4 current. The means \pm standard deviations from four experiments are indicated.

30 °C was critical to the detection of the HCN4-dependent inward current, as reported for several ion channels.^{39,40} All subsequent experiments were performed using HCN4-expressing CHO cells incubated at 30 °C before measurements. The current trace of HCN4 could be fitted to a monophasic exponential with a slow tau component (813.6 ms; **Fig. 1A**, bottom left), indicating that HCN4 had no inactivation state during the 5 s pulse, as reported in the literature using conventional patch clamping.^{41,42} The $V_{1/2}$ value obtained was -94.9 ± 5.9 mV (**Fig. 1B**), which was also in good agreement with previous reports based on conventional patch-clamping systems.^{41,43} To confirm the properties of well-known HCN blockers, we designed a voltage protocol composed of six repetitive hyperpolarization pulses with a focus on the detection of use-dependent blockade (**Fig. 2A**, top). Depolarization steps to accelerate the closing of HCN4 channels were adopted at each end of the hyperpolarization pulse, based on the literature.²⁴ **Figure 2A** shows the typical traces recorded as HCN4 currents, as well as those obtained in the presence of the HCN4 blockers ivabradine and ZD7288. Although the two HCN4 blockers diminished the HCN4 current in a concentration-dependent manner, ivabradine alone afforded an increase in blockade according to pulse number, that is, use-dependent blockade (**Fig. 2A,B**), which was in accordance with a previous report.²⁴ As we observed that a final DMSO concentration >1% in the wells decreased the HCN4 current (**Fig. 2C**), for the compound evaluation performed here, the crossover of DMSO from test compounds was adjusted as 0.3% in each well in all experiments.

We then conducted a random screening of ~16,000 compounds in our small-molecule compound library at 30 μ M. The first half of the screening was performed in an SH mode, and the second half was performed in a PPC mode, thus enabling a higher throughput. The success rate of all studies was approximately 80%–95% (see Materials and Methods for the success criteria). A histogram displaying the distribution of the percent inhibition values in the sample wells is provided in **Figure 3A**; some correspondence to a normal distribution with broad tails was observed. After the confirmation of reproducibility for 1200 compounds with more than 30% inhibition at 30 μ M, intracellular cAMP was measured in hHCN4-expressing cells incubated in the presence of the compounds, to eliminate those that regulate cAMP signaling, because intracellular cAMP directly regulates HCN4 activity;^{44,45} however, this concern was proven to be unfounded (data not shown). We finally identified 189 compounds showing more than 50% inhibitory effects on HCN4 without significant intracellular cAMP suppression at 30 μ M. Among these, we focused on three novel hit compounds, namely, T-478, T-788, and T-524 (**Fig. 3B**), which were distinct from both ivabradine and ZD7288 in structures. Interestingly, their blockade traces were diverse, as shown in **Figure 3C**; T-478, similar

to ivabradine, showed use-dependent blockade, while T-788, T-524, and ZD7288, repetitively, exhibited almost the same blockade or even a decreasing blockade over six pulses. Of note, the use-dependent blockade of T-478 reached the equivalent faster within the first two or three pulses in this condition, while the blockade afforded by ivabradine was increased further at the sixth pulse.

Next, we applied a longer hyperpolarization protocol to profile these blockers. The test pulse and typical traces are shown in **Figure 4A** (top left and the others, respectively). The group composed of T-478 and ivabradine was obviously distinguishable from that composed of T-788, T-524, and ZD7288 regarding the traces, especially in an earlier phase (between 1000 and 5000 ms), as shown in **Figure 4A**. Moreover, the blocking kinetics of T-788 was slightly different from that of T-524. While the blockade of T-524 reached a plateau with a significant remaining current, the blockade of T-788 showed no plateau phase and almost disappeared. To evaluate quantitatively the blocking kinetics, the inhibition rate was calculated at each predetermined time after the onset of the hyperpolarization pulse. As shown in **Figure 4B**, T-478 weakly blocked the HCN4 current at 1000 ms after the onset of the hyperpolarization pulse, whereas the blockade drastically increased with the prolongation of the hyperpolarization up to 9500 ms. Centrally, the ivabradine-induced blockade increased only slightly with prolonged hyperpolarization. Conversely, the blocking potency of T-788 reached a maximum value at 1500 ms after the onset of the hyperpolarization pulse, and then decreased in the presence of a prolonged hyperpolarization of up to 9500 ms. T-524 and ZD7288 also showed strong blockade at 1000 ms after the onset of the hyperpolarization pulse, and the inhibition curves shifted rightward in a concentration-dependent manner in the presence of a prolonged hyperpolarization, although the shifts were much smaller than those observed for T-788.

These variable kinetics might imply the diversity of the binding sites of HCN4. Therefore, we next performed a site-directed mutagenesis experiment to gain molecular insights into the amino acid residues of HCN4 that participate in the binding to the blockers. hERG, which is a close homolog of HCN channels, has been well investigated in drug discovery aimed at the development of drugs without toxic hERG blockade.^{46,47} A variety of amino acid residues have been indicated to bind to hERG blockers.^{48,49} For example, S624, which is located at a selective filter facing the inner cavity of the channel, is critical for some representative hERG blockers, that is, dofetilide and E4031, while Y652 and Y656, which are both located at the inner side of the middle part of the S6 loop, are also known as important residues for other blockers, such as cisapride.⁴⁹ By reference to the alignment of the amino acid sequences of human HCN4 and hERG channels, we chose residues C478, Y506, and I510 of HCN4, which correspond to residues S624,

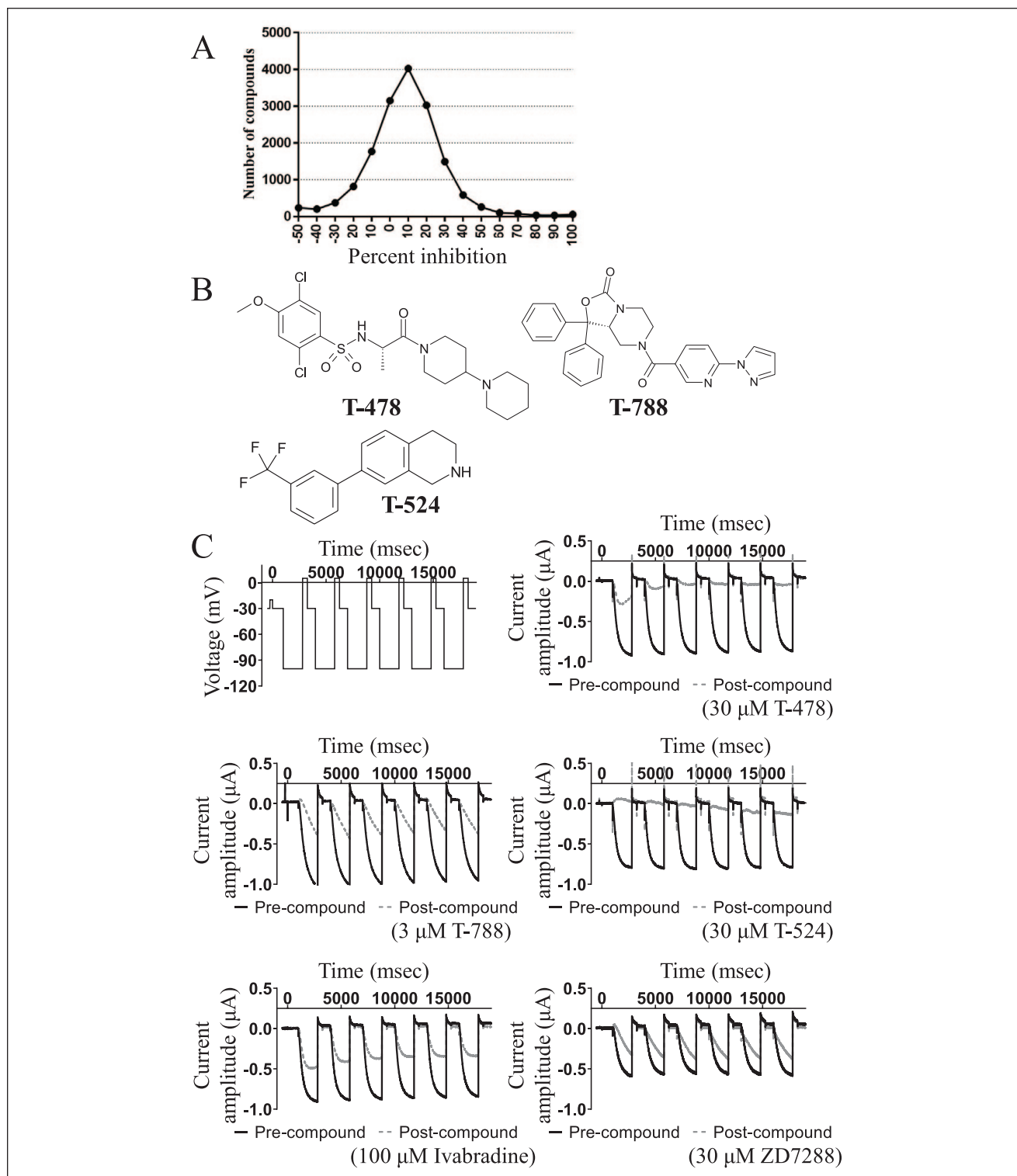


Figure 3. Results of the HCN4 chemical screening campaign. **(A)** Histogram displaying the distribution of the percent of inhibition values in the sample wells in a primary screen of ~16,000 small-molecule compounds at 30 μ M. The average and standard deviation of the percentage of inhibition were 8.6% and 20.6%, respectively. **(B)** Chemical structures of the three hit compounds, termed T-478, T-788, and T-524, analyzed in this report. **(C)** Six-pulse voltage protocol (top left) and typical current traces recorded before compound addition (pre-compound) and after the addition of each compound (postcompound). The test protocol was slightly modified from **Figure 2A**, to maximize the success rate of detecting HCN4 signals. The representative traces from T-478 (30 μ M), T-788 (3 μ M), T-524 (30 μ M), ivabradine (100 μ M), and ZD7288 (30 μ M) are presented.

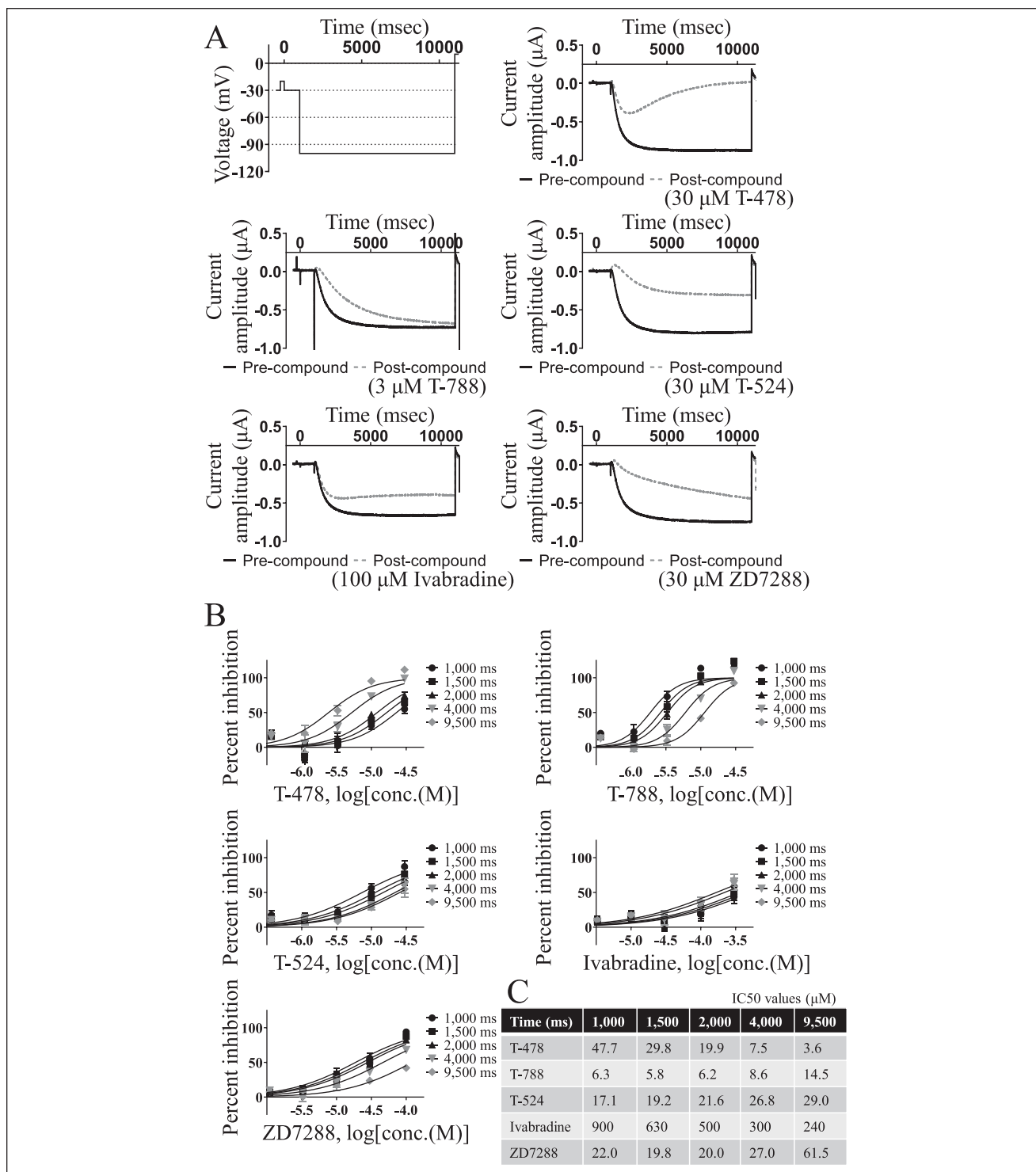


Figure 4. Analysis of HCN4-blocking kinetics by the three hit compounds, ivabradine, and ZD7288 under prolonged pulses. **(A)** One-long-pulse protocol (top left) and typical current traces recorded before compound addition (precompound) and after the addition of each compound (postcompound). The representative traces from T-478 (30 μM), T-788 (3 μM), T-524 (30 μM), ivabradine (100 μM), and ZD7288 (30 μM) are presented. The concentrations that showed the most typical blocking kinetics in this protocol were selected. **(B)** Concentration-dependent blockade of the HCN4 channel by the three hit compounds, ivabradine, and ZD7288 at the indicated time points after the onset of the hyperpolarization. Current amplitudes were detected at the indicated time points after the onset of the hyperpolarization pulse. The means \pm standard errors of the mean from four experiments are indicated. **(C)** Table of the IC₅₀ values obtained in **B**.

Y652, and F656 in hERG, respectively, and introduced site-directed mutations for switching them to alanine residues (**Fig. 5A**). The currents of the C478A or Y506A mutants of HCN4 were successfully measured using IonWorks in a PPC mode. Because cells transfected with the I510A mutant of HCN4 showed small amplitudes of the HCN4 current, which was also reported by a previous study,⁵⁰ we measured the current of the I510A mutant of HCN4 in an SH mode, as this was more suitable for recordings of smaller-amplitude currents.^{30,51} The blockade of the HCN4 current by T-478 and ivabradine was significantly diminished in the C478A mutant (**Fig. 5B**). This suggests that the C478 residue is at least partly critical for the binding of T-478 and ivabradine. Moreover, Y506 was the site that affected the blocking potency of T-478, but not of ivabradine. Regarding other blockers, Y506 was involved in the blocking potency of ZD7288. The remaining two blockers, T-788 and T-524, drastically depended on I510, rather than Y506.

Discussion

We report here the results of a compound screening campaign for HCN4 blockers, the identification of novel HCN4 blockers, and the unique blocking kinetics and binding properties of the novel HCN4 blockers, which were obtained using an automated patch-clamp device, IonWorks. Notably, this was the first report of HTS for HCN4 blockers from a compound library containing as many as 16,000 compounds and using an automated patch-clamp system, which enabled us to identify novel HCN4 blockers.

In the PPC mode, the researcher can detect the total ensemble of the currents produced by cells on a well with 64 holes; in this way, the success rate of the recording in the screening obtained in our study was as high as 80%–95%. We were able to evaluate ~1400 compounds/day, which was sufficient to explore hit compounds in random screenings. It is generally recognized that the PPC mode in an automated patch clamp is not suitable for kinetics analysis because the loose seal resistance caused by the multiholes dampens the voltage loads.^{27,29,30} However, greater uniformity and subsequent minimalizations of well-to-well differences in the PPC mode were effective in comparing the recorded kinetics among compounds. In fact, we could clearly distinguish the blocking kinetics of T-478 and ivabradine from those of the other blockers in an earlier phase (between 1000 and 5000 ms), and the kinetics of T-788 from those of T-524 in a plateau phase (**Fig. 4A,B**). The PPC mode is not suitable for detecting the accurate time constants of channels with rapid kinetics, but can be available for comparing current traces affected by various compounds in slow-kinetics channels, such as HCNs.

HCN4 blockers with various blocking properties should be helpful to explore the relationship between the molecular behaviors of HCN4 and SAN activities in the heart. Previous

studies suggested that the use dependence resulting from the specific features of the ivabradine-induced blockade probably contributed to its slow developing effect in isolated normal SANs and to its increased rate-reducing ability at higher spontaneous rates, which may be beneficial for clinical applications.^{24,52} The blocking kinetics of T-478 was unique because the increase of its blockade during the hyperpolarization pulse was obviously even larger than that of ivabradine (**Fig. 4A–C**). Comparing the effects of T-478 and ivabradine on SAN activities at high and low spontaneous rates in *in vivo* studies might be valuable. In addition, the blocking kinetics of T-788 was unique because its blockade dramatically decreased when the hyperpolarization pulse was prolonged (**Fig. 4A,B**). Furthermore, T-524 showed similar blocking kinetics with T-788 and ZD7288, but the blockade of T-524 reached a plateau with a significant remaining current varying from those of others (**Fig. 4A**), and a lower concentration of T-524 (10 μM) also showed a plateau phase (data not shown), which might affect the pharmacological efficacy in SAN activities. Indeed, all three compounds (T-478, T-788, T-524) reduced heart rate in isolated rat right atrium *in vitro* (data not shown), and further detailed functional studies may be valuable.

In an IonWorks instrument, compounds are preloaded before the test pulse,³⁸ leading to the interpretation that T-788 might be a closed-state channel-specific blocker and that T-524 might be a closed-state and open-state channel blocker. However, a recent cryo-electron microscopy structural analysis of HCN1 revealed that the pore cavity was too tight for ivabradine or other compounds to enter the pore space in the closed state of HCN1.⁵³ Moreover, previous studies demonstrated that ivabradine and ZD7288 are open-state channel blockers for HCN4 depending on the current amplitudes of K^+ influx, as their binding to HCN4 is conflicted and “kicked off” by the K^+ influx.^{23,52} Taken together, T-788 and T-524 possibly exhibit potent inhibition just after the channel opens (0 to 1000 ms) and might then be pushed away by the strong hyperpolarization or the subsequent large K^+ entry. Unfortunately, IonWorks has limitations in recording current under small K^+ influx due to its low signal-to-background ratio, and it is not possible to apply test compounds under voltage clamping conditions, so that further analysis of the mode of action is necessary using the conventional patch-clamp methods or other instruments, in which giga seals and on-time test-compound applications to the preopened HCN4 channels are available. Further studies under such “gold-standard” conditions also aid in assessing kinetic parameters, such as time constants, among these HCN4 blockers.

A mutagenetic analysis was subsequently performed to explore the molecular binding sites of hHCN4. By reference to the alignment of the amino acid sequences of the hHCN4 and hERG channels,⁴⁹ we chose residues C478,

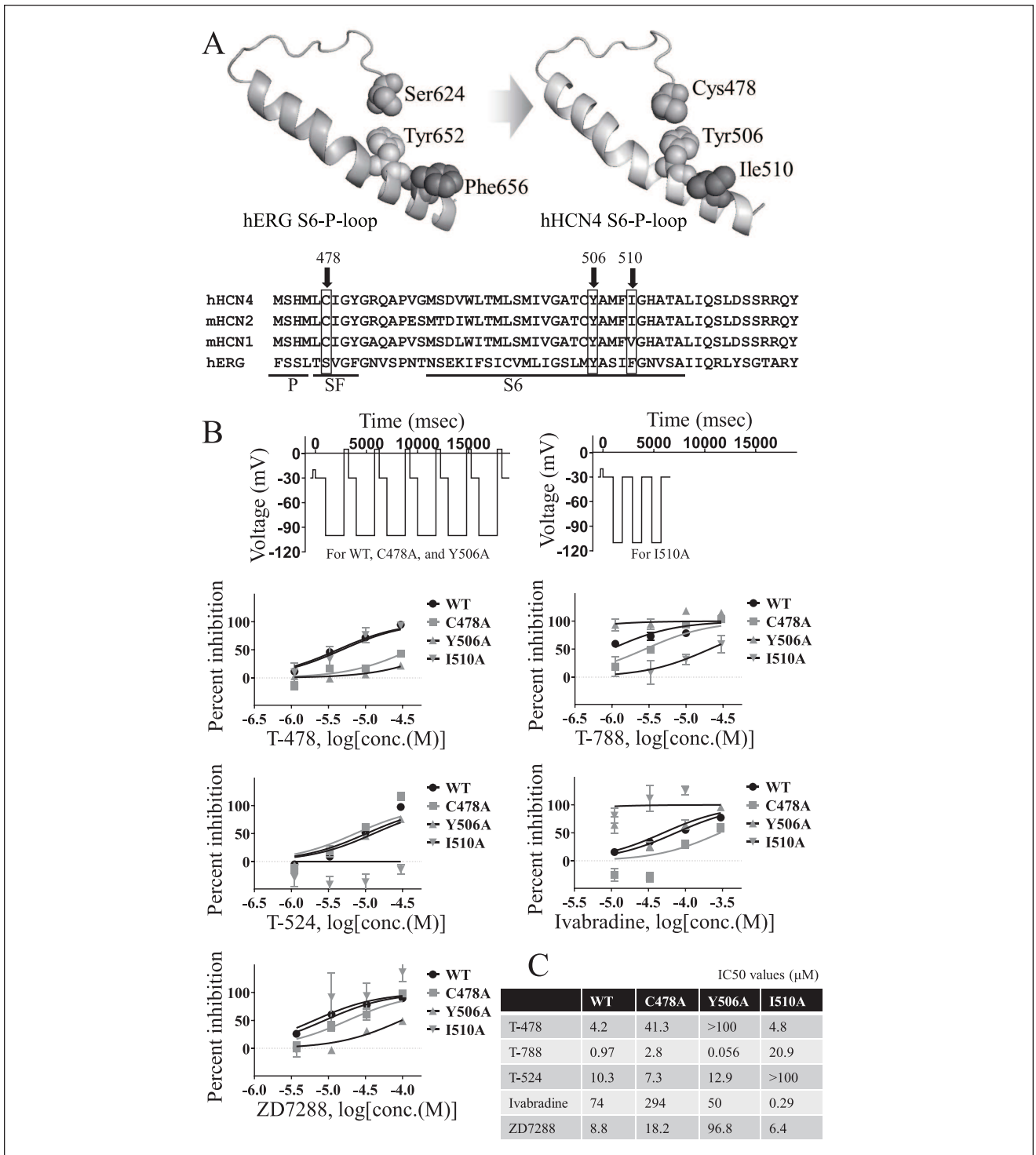


Figure 5. Mutagenetic analysis of the three hit compounds, ivabradine, and ZD7288. **(A)** Schematic representation of the S6-P loops in hERG and hHCN4. The corresponding amino acid residues that were mutated in this report are indicated. Multiple sequence alignment of the S6-P loop of hHCN4 with the corresponding regions of mHCN2, mHCN1, and hERG is also shown. The mutated amino acid residues in hHCN4 and corresponding ones in others are indicated by arrows. P = pore, SF = selectivity filter. **(B)** Concentration-dependent blockade by the three hit compounds, ivabradine, and ZD7288 of the currents of wild-type (WT), C478A, Y506A, and I510A HCN4. The voltage protocols used for the WT, C478A, and Y506A mutants (top left, same as Fig. 3C) and one for I510A (top right, three-pulse protocol without depolarization steps to maximize the success rate of signal detection) are shown. The means ± standard errors of the mean from 16 experiments are indicated. **(C)** Table of the IC50 values obtained in B.

Y506, and I510 of HCN4 as the residues for the mutagenesis analysis (Fig. 5A). Regarding ZD7288, Y506 was identified as a necessary residue for its binding, while C478 and I510 were not (Fig. 5B,C). This result contradicted those of previous studies of other HCN subtypes; Chan et al. identified contributions of all three corresponding residues in mouse HCN1, and Cheng et al. clarified the importance of the mouse HCN2 residue corresponding to I510, but not of that corresponding to C478 or Y506.^{54,55} A recent study of a docking model suggested that ZD7288 is relatively free to rotate within the pore cavity of HCN1.⁵⁶ It seems that chemical orientation and molecular binding sites for ZD7288 might be different in each isoform of HCNs. In turn, C478 was the most critical residue for binding to ivabradine (Fig. 5B,C), which was unexpected because Bucchi et al. demonstrated through mutagenesis studies that Y506 and I510, but not C478, are important for the binding of ivabradine to hHCN4.⁵⁰ They studied the ivabradine-induced blockade of the hHCN4 current induced by hyperpolarization at -140 mV, rather than the -100 mV used in this work. Moreover, the intensity of the K^+ flow and/or the membrane potential might affect the chemical orientation and binding site of ivabradine. The number of repetitive pulses was also different among the studies. Thus, it is possible that the differences in assay conditions contributed to this discrepancy. Considering the possibility that the mutagenetic approach tends to depend on HCN subtypes and assay conditions, even for the same channel, care should be taken to unify the conditions and protocols when comparing the profiles of several test compounds. Unexpectedly, Y506A and I510A significantly increased the potency of T-788 and ivabradine, respectively (Fig. 5B,C). Although the cause is not clear, it is possible that the steric coordinates of other amino acid side chains might be changed by the mutation, resulting in increased affinity. Alternatively, alanine substitution may reduce steric hindrance. The mechanism of increased inhibitory activity in mutants should be further investigated.

In the present study, T-788, T-524, and ZD7288, which exhibit a weakened potency when the channel is open, did not rely on the amino acid residue C478 but on residues Y506 or I510, which are located at the inner side of the S6 loop in the pore cavity. A recent structural analysis of hERG and KvChim demonstrated that the hERG pore around Y652 and F656, corresponding to Y506 and I510 in hHCN4, was expanded from 1 \AA to more than 5 \AA in the open state.⁵⁷ Based on the hypothesis of the drastic spread of the pores around the inner side of the gates in HCN4, it is reasonable to think that channel opening would disrupt the binding and critically attenuate the potency of these compounds. Conversely, T-478 and ivabradine exhibited preferred binding to C478 in our study. C478 is a residue located in the selective filter and its structural changes are thought to be limited, even during channel opening. Interacting with C478 at the cell-surface side in the pore groove might be

advantageous for keeping its affinity, to tolerate structural alterations under channel opening; moreover, considering that T-478 and ivabradine exhibited use-dependent blockade, interacting with C478 would probably also be beneficial for use-dependent blockade.

This study demonstrated the existence of a variety of novel binding kinetics and binding properties among HCN4 blockers. These novel compounds with unique profiles will promote the biomolecular and pharmacological understanding of the HCN4 channel in the heart and may contribute to the expansion of therapeutic options in the future.

Acknowledgments

The authors would like to express their great appreciation to Shinji Moriyama and Michiyo Tokuhara for accurately conducting HTS and mutagenesis studies using IonWorks. Special thanks go to Kenichi Imahashi for helpful discussion regarding the mechanism of HCN4 blockade as a skilled specialist in cardiovascular diseases, Yumi N. Imai for deep insights into structural biology and useful discussions, and Hiroki Sakamoto for significant contribution to valuable and well-aimed discussion and test compound selection.

Declaration of Conflicting Interests

The authors declared the following potential conflicts of interest with respect to the research, authorship, and/or publication of this article: All authors are employed by Takeda Pharmaceutical, and their research and authorship of this article were completed within the scope of their employment with Takeda Pharmaceutical.

Funding

The authors disclosed receipt of the following financial support for the research, authorship, and/or publication of this article: This research was funded by Takeda and received no specific grant from any funding agency in the public, commercial, or not-for-profit sectors.

ORCID iD

Kosuke Nakashima  <https://orcid.org/0000-0002-4835-0953>

References

1. Biel, M.; Ludwig, A.; Zong, X.; et al. Hyperpolarization-Activated Cation Channels: A Multi-Gene Family. *Rev. Physiol. Biochem. Pharmacol.* **1999**, *136*, 165–181.
2. Kaupp, U. B.; Seifert, R. Molecular Diversity of Pacemaker Ion Channels. *Annu. Rev. Physiol.* **2001**, *63*, 235–257.
3. Ludwig, A.; Budde, T.; Stieber, J.; et al. Absence Epilepsy and Sinus Dysrhythmia in Mice Lacking the Pacemaker Channel HCN2. *EMBO J.* **2003**, *22*, 216–224.
4. Santoro, B.; Tibbs, G. R. The HCN Gene Family: Molecular Basis of the Hyperpolarization-Activated Pacemaker Channels. *Ann. N.Y. Acad. Sci.* **1999**, *868*, 741–764.
5. Benarroch, E. E. HCN Channels: Function and Clinical Implications. *Neurology* **2013**, *80*, 304–310.

6. DiFrancesco, D. Characterization of Single Pacemaker Channels in Cardiac Sino-Atrial Node cells. *Nature* **1986**, *324*, 470–473.
7. DiFrancesco, D. The Role of the Funny Current in Pacemaker Activity. *Circ. Res.* **2010**, *106*, 434–446.
8. Robinson, R. B.; Siegelbaum, S. A. Hyperpolarization-Activated Cation Currents: From Molecules to Physiological Function. *Annu. Rev. Physiol.* **2003**, *65*, 453–480.
9. Wahl-Schott, C.; Biel, M. HCN Channels: Structure, Cellular Regulation and Physiological Function. *Cell. Mol. Life Sci.* **2009**, *66*, 470–494.
10. Sartiani, L.; Mannaioni, G.; Masi, A.; et al. The Hyperpolarization-Activated Cyclic Nucleotide-Gated Channels: From Biophysics to Pharmacology of a Unique Family of Ion Channels. *Pharmacol. Rev.* **2017**, *69*, 354–395.
11. Zhuang, Q. X.; Li, G. Y.; Li, B.; et al. Regularizing Firing Patterns of Rat Subthalamic Neurons Ameliorates Parkinsonian Motor Deficits. *J. Clin. Invest.* **2018**, *128*, 5413–5427.
12. Raghunathan, S.; Islas, J. F.; Mistretta, B.; et al. Conversion of Human Cardiac Progenitor Cells into Cardiac Pacemaker-Like Cells. *J. Mol. Cell. Cardiol.* **2019**, *138*, 12–22.
13. Santoro, B.; Shah, M. M. Hyperpolarization-Activated Cyclic Nucleotide-Gated Channels as Drug Targets for Neurological Disorders. *Annu. Rev. Pharmacol. Toxicol.* **2020**, *60*, 109–131.
14. Andrikopoulos, G.; Dasopoulou, C.; Sakellariou, D.; et al. Ivabradine: A Selective If Current Inhibitor in the Treatment of Stable Angina. *Recent Pat. Cardiovasc. Drug Discov.* **2006**, *1*, 277–282.
15. Cargnoni, A.; Ceconi, C.; Stavroula, G.; et al. Heart Rate Reduction by Pharmacological If Current Inhibition. *Adv. Cardiol.* **2006**, *43*, 31–44.
16. Fox, K.; Ford, I.; Steg, P. G.; et al. Ivabradine for Patients with Stable Coronary Artery Disease and Left-Ventricular Systolic Dysfunction (BEAUTIFUL): A Randomised, Double-Blind, Placebo-Controlled Trial. *Lancet* **2008**, *372*, 807–816.
17. Swedberg, K.; Komajda, M.; Bohm, M.; et al. Ivabradine and Outcomes in Chronic Heart Failure (SHIFT): A Randomised Placebo-Controlled Study. *Lancet* **2010**, *376*, 875–885.
18. BoSmith, R. E.; Briggs, I.; Sturgess, N. C. Inhibitory Actions of ZENECA ZD7288 on Whole-Cell Hyperpolarization Activated Inward Current (If) in Guinea-Pig Dissociated Sinoatrial Node Cells. *Br. J. Pharmacol.* **1993**, *110*, 343–349.
19. He, J. T.; Li, X. Y.; Zhao, X.; et al. Hyperpolarization-Activated and Cyclic Nucleotide-Gated Channel Proteins as Emerging New Targets in Neuropathic Pain. *Rev. Neurosci.* **2019**, *30*, 639–649.
20. Cao, Y.; Chen, S.; Liang, Y.; et al. Inhibition of Hyperpolarization-Activated Cyclic Nucleotide-Gated Channels by Beta-Blocker Carvedilol. *Br. J. Pharmacol.* **2018**, *175*, 3963–3975.
21. Tamura, A.; Ogura, T.; Uemura, H.; et al. Effects of Antiarrhythmic Drugs on the Hyperpolarization-Activated Cyclic Nucleotide-Gated Channel Current. *J. Pharmacol. Sci.* **2009**, *110*, 150–159.
22. Cao, Y.; Pang, J.; Zhou, P. HCN Channel as Therapeutic Targets for Heart Failure and Pain. *Curr. Topics Med. Chem.* **2016**, *16*, 1855–1861.
23. Bucchi, A.; Tognati, A.; Milanese, R.; et al. Properties of Ivabradine-Induced Block of HCN1 and HCN4 Pacemaker Channels. *J. Physiol.* **2006**, *572*, 335–346.
24. Thollon, C.; Bedut, S.; Villeneuve, N.; et al. Use-Dependent Inhibition of hHCN4 by Ivabradine and Relationship with Reduction in Pacemaker Activity. *Br. J. Pharmacol.* **2007**, *150*, 37–46.
25. Shin, K. S.; Rothberg, B. S.; Yellen, G. Blocker State Dependence and Trapping in Hyperpolarization-Activated Cation Channels: Evidence for an Intracellular Activation Gate. *J. Gen. Physiol.* **2001**, *117*, 91–101.
26. Meng, Q. T.; Xia, Z. Y.; Liu, J.; et al. Local Anesthetic Inhibits Hyperpolarization-Activated Cationic Currents. *Mol. Pharmacol.* **2011**, *79*, 866–873.
27. Farre, C.; Stoelzle, S.; Haarmann, C.; et al. Automated Ion Channel Screening: Patch Clamping Made Easy. *Expert Opin. Ther. Targets* **2007**, *11*, 557–565.
28. McManus, O. B. HTS Assays for Developing the Molecular Pharmacology of Ion Channels. *Curr. Opin. Pharmacol.* **2014**, *15*, 91–96.
29. Milligan, C. J.; Moller, C. Automated Planar Patch-Clamp. *Methods Mol. Biol.* **2013**, *998*, 171–187.
30. Priest, B. T.; Cerne, R.; Krambis, M. J.; et al. Automated Electrophysiology Assays. In *Assay Guidance Manual*; Sittampalam, G. S., Grossman, A., Brimacombe, K.; et al., Eds.; Eli Lilly & Company and the National Center for Advancing Translational Sciences: Bethesda, MD, **2004**.
31. Harmer, A. R.; Abi-Gerges, N.; Easter, A.; et al. Optimisation and Validation of a Medium-Throughput Electrophysiology-Based hNav1.5 Assay Using IonWorks. *J. Pharmacol. Toxicol. Methods* **2008**, *57*, 30–41.
32. Trivedi, S.; Dekermendjian, K.; Julien, R.; et al. Cellular HTS Assays for Pharmacological Characterization of Na(V)1.7 Modulators. *Assay Drug Dev. Technol.* **2008**, *6*, 167–179.
33. Obergrussberger, A.; Brüggemann, A.; Goetze, T. A.; et al. Automated Patch Clamp Meets High-Throughput Screening: 384 Cells Recorded in Parallel on a Planar Patch Clamp Module. *J. Lab. Autom.* **2016**, *21*, 779–793.
34. Bell, D. C.; Dallas, M. L. Using Automated Patch Clamp Electrophysiology Platforms in Pain-Related Ion Channel Research: Insights from Industry and Academia. *Br. J. Pharmacol.* **2018**, *175*, 2312–2321.
35. Obergrussberger, A.; Goetze, T. A.; Brinkwirth, N.; et al. An Update on the Advancing High-Throughput Screening Techniques for Patch Clamp-Based Ion Channel Screens: Implications for Drug Discovery. *Expert Opin. Drug Discov.* **2018**, *13*, 269–277.
36. Walsh, K. B. Screening Technologies for Inward Rectifier Potassium Channels: Discovery of New Blockers and Activators. *SLAS Discov.* **2020**, *25*, 420–433.
37. Obergrussberger, A.; Friis, S.; Brüggemann, A.; et al. Automated Patch Clamp in Drug Discovery: Major Breakthroughs and Innovation in the Last Decade. *Expert Opin. Drug Discov.* **2021**, *16*, 1–5.
38. Schroeder, K.; Neagle, B.; Trezise, D. J.; et al. IonWorks HT: A New High-Throughput Electrophysiology Measurement Platform. *J. Biomol. Screen.* **2003**, *8*, 50–64.

39. Goehring, A.; Lee, C. H.; Wang, K. H.; et al. Screening and Large-Scale Expression of Membrane Proteins in Mammalian Cells for Structural Studies. *Nat. Protoc.* **2014**, *9*, 2574–2585.
40. Wright, P. D.; Kanumilli, S.; Tickle, D.; et al. A High-Throughput Electrophysiology Assay Identifies Inhibitors of the Inwardly Rectifying Potassium Channel Kir7.1. *J. Biomol. Screen.* **2015**, *20*, 739–747.
41. Ludwig, A.; Zong, X.; Stieber, J.; et al. Two Pacemaker Channels from Human Heart with Profoundly Different Activation Kinetics. *EMBO J.* **1999**, *18*, 2323–2329.
42. Michels, G.; Er, F.; Khan, I.; et al. Single-Channel Properties Support a Potential Contribution of Hyperpolarization-Activated Cyclic Nucleotide-Gated Channels and If to Cardiac Arrhythmias. *Circulation* **2005**, *111*, 399–404.
43. Qu, J.; Altomare, C.; Bucchi, A.; et al. Functional Comparison of HCN Isoforms Expressed in Ventricular and HEK 293 Cells. *Pflugers Arch.* **2002**, *444*, 597–601.
44. Seifert, R.; Scholten, A.; Gauss, R.; et al. Molecular Characterization of a Slowly Gating Human Hyperpolarization-Activated Channel Predominantly Expressed in Thalamus, Heart, and Testis. *Proc. Natl. Acad. Sci. U.S.A.* **1999**, *96*, 9391–9396.
45. Wainger, B. J.; DeGennaro, M.; Santoro, B.; et al. Molecular Mechanism of cAMP Modulation of HCN Pacemaker Channels. *Nature* **2001**, *411*, 805–810.
46. Sanguinetti, M. C.; Tristani-Firouzi, M. hERG Potassium Channels and Cardiac Arrhythmia. *Nature* **2006**, *440*, 463–469.
47. Vandenberg, J. I.; Perry, M. D.; Perrin, M. J.; et al. hERG K(+) Channels: Structure, Function, and Clinical Significance. *Physiol. Rev.* **2012**, *92*, 1393–1478.
48. Perry, M.; Stansfeld, P. J.; Leaney, J.; et al. Drug Binding Interactions in the Inner Cavity of HERG Channels: Molecular Insights from Structure-Activity Relationships of Clofilium and Ibutilide Analogs. *Mol. Pharmacol.* **2006**, *69*, 509–519.
49. Stansfeld, P. J.; Gedeck, P.; Gosling, M.; et al. Drug Block of the hERG Potassium Channel: Insight from Modeling. *Proteins* **2007**, *68*, 568–580.
50. Bucchi, A.; Baruscotti, M.; Nardini, M.; et al. Identification of the Molecular Site of Ivabradine Binding to HCN4 Channels. *PLoS One* **2013**, *8*, e53132.
51. Finkel, A.; Wittel, A.; Yang, N.; et al. Population Patch Clamp Improves Data Consistency and Success Rates in the Measurement of Ionic Currents. *J. Biomol. Screen.* **2006**, *11*, 488–496.
52. Bucchi, A.; Baruscotti, M.; DiFrancesco, D. Current-Dependent Block of Rabbit Sino-Atrial Node I(f) Channels by Ivabradine. *J. Gen. Physiol.* **2002**, *120*, 1–13.
53. Lee, C. H.; MacKinnon, R. Structures of the Human HCN1 Hyperpolarization-Activated Channel. *Cell* **2017**, *168*, 111–120.e111.
54. Chan, Y. C.; Wang, K.; Au, K. W.; et al. Probing the Bradycardic Drug Binding Receptor of HCN-Encoded Pacemaker Channels. *Pflugers Arch.* **2009**, *459*, 25–38.
55. Cheng, L.; Kinard, K.; Rajamani, R.; et al. Molecular Mapping of the Binding Site for a Blocker of Hyperpolarization-Activated, Cyclic Nucleotide-Modulated Pacemaker Channels. *J. Pharmacol. Exp. Ther.* **2007**, *322*, 931–939.
56. Tanguay, J.; Callahan, K. M.; D'Avanzo, N. Characterization of Drug Binding within the HCN1 Channel Pore. *Sci. Rep.* **2019**, *9*, 465.
57. Wang, W.; MacKinnon, R. Cryo-EM Structure of the Open Human Ether-a-Go-Go-Related K(+) Channel hERG. *Cell* **2017**, *169*, 422–430.e410.